Proceedings of the Second Joint EMBS/BMES Conference
Houston, TX, USA • October 23-26, 2002

Regularized Approach in 3D Helical Computed Tomography

M. Allain[1,2], Y. Goussard[1], J. Idier[2]
[1]École Polytechnique de Montréal, Montréal (Québec), Canada
[2]Laboratoire des Signaux et Systèmes - CNRS-Supélec-UPS, Gif-sur-Yvette, France

Abstract- **Helical tomography yields less invasive examination at the expense of degradations in the precision of the reconstructions and the possible presence of specific artifacts. This study presents a new reconstruction method that produces significant enhancement in the precision of helical tomographic images at a reasonable computer cost.**
Keywords- **Helical tomography, penalized least-square, 3D reconstruction algorithm.**

I. Introduction

X-ray computed tomography (CT) is a fast and mildly invasive technique that produces three-dimensional (3D) images from a set of projections. In *planar geometry*, the volume is produced by stacking a series of slices reconstructed from two-dimensional (2D) data. Although the precision of such a reconstruction technique is often sufficient for safe medical diagnosis, it remains insufficient to achieve accurate quantitative measurements [1]. In the past ten years, planar scanners have been massively replaced by *helical scanners* that reduce the scanning time as well as the radiation dose sent to the patient. However, the price to pay for such gains is a loss in the accuracy of the images and the possible presence of strong artifacts. These effects result in part from *ad hoc* interpolation procedures[1] introduced in order to use the standard planar *convolution backprojection* (CBP) reconstruction algorithm.

This paper presents a new reconstruction method based on an *algebraic* formulation of helical tomography in its natural 3D setting. A *regularization* framework is used to deal with the well-known *ill-posed* nature of the reconstruction problem. This approach brings significant enhancement to the precision of helical tomographic reconstruction at a reasonable computer cost.

II. Methodology

We address the problem in a discrete framework; let $\boldsymbol{f} \in \mathbb{R}^N$ and $\boldsymbol{p}_h \in \mathbb{R}^{N_m}$ respectively denote the original 3D scene and the raw data vector that contains the whole set of projections in helical geometry. Our goal is to compute an *estimate* $\widehat{\boldsymbol{f}}$ of $\boldsymbol{f}$. Our approach to reconstruction relies on the minimization of a penalized least-square criterion: firstly, a model $\mathcal{H}(\boldsymbol{f})$ of the helical projection process is constructed and secondly, the regularized estimate $\widehat{\boldsymbol{f}}$ is defined as the minimizer of:

$$J(\boldsymbol{f}) = \|\mathcal{H}(\boldsymbol{f}) - \boldsymbol{p}_h\|^2 + \lambda\Phi(\boldsymbol{f}) \quad \lambda \geq 0, \tag{1}$$

where Φ corresponds to a prior model. Parameter λ weights the two terms of the criterion. Difficulties encountered in minimizing (1) are deeply connected to the specificities of models $\mathcal{H}$ and Φ. In the next section, it is shown that under standard assumptions, $\mathcal{H}$ can be given a simple structural form.

A. Model in helical tomography

In planar geometry, it is commonly assumed that the projection data are linked to the object through a sparse linear operator $\boldsymbol{W}$ which approximates a 2D discrete Radon transform [2]. Then, a given projection at angle θ_j corresponds to a submatrix $\boldsymbol{W}_j$ extracted from $\boldsymbol{W}$. We now extend this standard projection model to 3D spiral geometry.

Let $\boldsymbol{f} = \{\boldsymbol{f}^k \in \mathbb{R}^L\}_{k=1}^K$ and (XYZ) respectively denote the 3D scene with K voxel slices and an axis system where OZ is the axis of the scanner. $\bar{\theta}_i \in \mathbb{R}$ is a projection angle on the helix. We assume without loss of generality that the axial ray width δ is not greater than the slice width. As a result, a projection from angle $\bar{\theta}_i$ in our model interacts with *at most* two slices, say $\boldsymbol{f}^k$ and $\boldsymbol{f}^{k+1}$, of respective proportions $\gamma_j^k \in (0;1]$ and $1-\gamma_j^k \equiv \bar{\gamma}_j^k$; see Fig. 1-(left). Let $\boldsymbol{p}^k$ gather the N_k projections associated with slices $(\boldsymbol{f}^k, \boldsymbol{f}^{k+1})$, and $\boldsymbol{\theta}^k \equiv \{\theta_j^k \in [0; 2\pi)\}_{j=1}^{N_k}$ be the

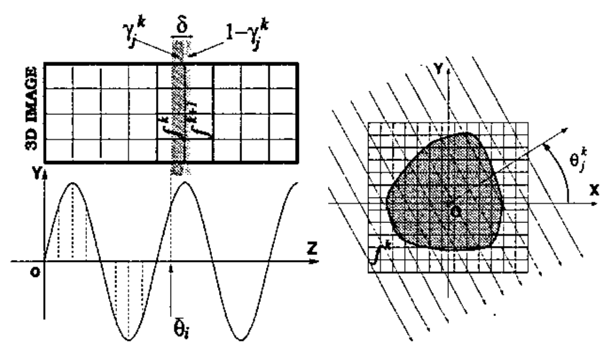

Fig. 1. Model in helical geometry: YOZ (left), XOY (right).

[1]Projections on the helix are interpolated in order to compose "pseudo sets" of projections in pre-determined axial planes.

corresponding set of projection angles. We get,

$$\boldsymbol{p}^k = \boldsymbol{H}^k \begin{bmatrix} \boldsymbol{f}^k \\ \boldsymbol{f}^{k+1} \end{bmatrix} \text{ with } \boldsymbol{H}^k = \begin{bmatrix} \gamma_1^k \boldsymbol{W}_1^k & \bar{\gamma}_1^k \boldsymbol{W}_1^k \\ \vdots & \vdots \\ \gamma_{N_k}^k \boldsymbol{W}_{N_k}^k & \bar{\gamma}_{N_k}^k \boldsymbol{W}_{N_k}^k \end{bmatrix} \qquad (2)$$

where $\boldsymbol{W}_j^k \in \mathbb{R}^{R \times L}$ is the projection operator in *planar geometry* associated to angle θ_j^k. Then, (2) yields *a linear model for helical tomography*: $\boldsymbol{p}_h = \mathcal{H}(\boldsymbol{f}) = \boldsymbol{H}\boldsymbol{f}$, with

$$\boldsymbol{p}_h = \begin{bmatrix} \boldsymbol{p}^1 \\ \vdots \\ \boldsymbol{p}^K \end{bmatrix}, \quad \boldsymbol{H} = \begin{bmatrix} \boxed{\boldsymbol{H}^1} & \boldsymbol{0} \dots & \boldsymbol{0} \\ \boldsymbol{0} & \boxed{\boldsymbol{H}^2} & \vdots \\ \vdots & \ddots & \boldsymbol{0} \\ \boldsymbol{0} & \cdots \boldsymbol{0} & \boxed{\boldsymbol{H}^K} \end{bmatrix} \in \mathbb{R}^{N_m \times N}. \quad (3)$$

Compared to planar geometry, helical geometry yields an intrinsically 3D model (L columns overlap between two adjacent blocks, each $\boldsymbol{H}^k$ being distinct in general). The resulting matrix $\boldsymbol{H}$ is huge (typically 10^{15} entries), and storing such a matrix would require an enormous memory capacity in spite of its strong sparsity. Here, we propose to circumvent this problem by assuming that *the helix pitch is an integer multiple P of the slice width.* Such an assumption can be met without loss of generality through appropriate axial sampling of the volume. Then, only P matrices $\boldsymbol{H}^k$ will suffice to describe $\boldsymbol{H}$, where K/P is about the number of helix turns.

B. L_2L_1 *regularization*

The image model Φ should convey relevant information about $\boldsymbol{f}$ without jeopardizing the computational feasibility of the minimization of J (1). We choose Φ so as to apply a L_2L_1 penalty to the differences in intensity values of neighboring voxels. Such models are well suited to the representation of objects composed of homogeneous areas separated by sharp discontinuities [1]. More specifically, we set $\Phi(\boldsymbol{f}) = \sum_c \phi(u_c\,; s)$ with $\phi(u_c\,; s) = \sqrt{u_c^2 + s^2}$ where $s > 0$ is a free scale parameter, and u_c ($c = 1, \cdots, M$) is the difference between a pair of adjacent voxels. We now show that such a model can yield a tractable image reconstruction method.

III. Inversion & results

Our choices yield the following expression of J:

$$J(\boldsymbol{f}) = \|\boldsymbol{p}_h - \boldsymbol{H}\boldsymbol{f}\|^2 + \lambda \textstyle\sum_{c=1}^{M} \sqrt{u_c^2 + s^2}. \qquad (4)$$

Although the minimizer of (4) cannot be expressed in closed form, the context remains favorable since J is C^1, convex and coercive. However, the huge size of this minimization problem ($\geq 10^6$ variables) precludes the use of standard methods (such as quasi-Newton), and derivation of an efficient algorithm with low numerical count is required. This can be achieved in the same manner as in [1], where a *Single Site Update* strategy is combined with the structural simplicity of the half-quadratic reformulation of J. The resulting algorithm has a very low computing cost and fast convergence. The performance of the method is illustrated in Fig. 2. A 3D synthetic phantom ($127 \times 127 \times 40$ voxels) was used to produce helical noisy (additive Gaussian white noise with zero mean and SNR=26 dB) projection data. Then "standard" reconstruction [3] based on *half-scan* interpolation and CBP, and L_2L_1 reconstruction were performed. Our results show significant improvements when the latter is used.

Estimating only a few slices of the volume or speeding up the reconstruction process is of great interest. Provided one accepts a moderate loss of accuracy, this can be done efficiently by successive *reduced* regularized reconstructions. The following approximation $\underline{\boldsymbol{p}}^k \approx \underline{\boldsymbol{H}}^k \underline{\boldsymbol{f}}^k$ based on (2) and (3) leads to the reduced regularized solution $\underline{\widetilde{\boldsymbol{f}}}^k$ defined as the minimizer of

$$J(\underline{\boldsymbol{f}}^k) = \|\underline{\boldsymbol{p}}^k - \underline{\boldsymbol{H}}^k \underline{\boldsymbol{f}}^k\|^2 + \lambda\Phi(\underline{\boldsymbol{f}}^k) \text{ with } \underline{\boldsymbol{f}}^k = \begin{bmatrix} \boldsymbol{f}^{k-1} \\ \boldsymbol{f}^k \\ \boldsymbol{f}^{k+1} \end{bmatrix} \qquad (5)$$

where $\underline{\boldsymbol{p}}^k$ and $\underline{\boldsymbol{H}}^k$ respectively gather the projections directly involved in slice k (*i.e.* $\boldsymbol{p}^{k-1}$ and $\boldsymbol{p}^k$) and the three blocks $\{\boldsymbol{H}^i\}_{i=k-1}^{k+1}$ under a structure similar to (3). Solving (5) yields $\widetilde{\boldsymbol{f}}^k$ which is a close approximation to $\widehat{\boldsymbol{f}}^k$, the k-th slice of $\widehat{\boldsymbol{f}}$. This technique decreases the computing cost by a factor of $K/3$ while the reconstruction remains accurate, as illustrated in Fig. 2.

References

[1] N. Villain et al., "Computed tomography image restoration using convex-potential 3-D Markov random fields", in *Proc. IEEE EMBS*, Chicago, IL, USA, 1997, pp. 561–564.

[2] A. C. Kak and M. Slaney, *Principles of Computerized Tomographic Imaging*, IEEE Press, New York, NY, 1988.

[3] C. R. Crawford and K. F. King, "Computed tomography scanning with simultaneous patient translation", *Med. Phys.*, vol. 17, no. 6, pp. 967–982, Jan. 1990.

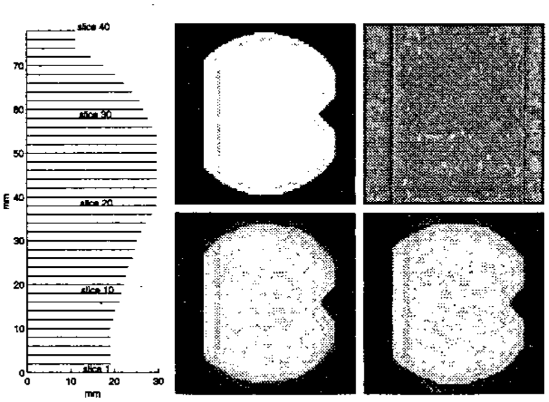

Fig. 2. [Up] - Phantom profile (OZ axis). [Down] - slice 19 (O): phantom, CBP + HS, optimal L_2L_1, fast L_2L_1.